

Chorus: Harmonizing Context and Sensing Signals for Data-Free Model Customization in IoT

Liyu Zhang, Yejia Liu, Kwun Ho Liu, Runxi Huang, Xiaomin Ouyang*
 Hong Kong University of Science and Technology
 {lzhangcx,yliutb,khliuae,rhuangbj}@connect.ust.hk,xmouyang@cse.ust.hk

ABSTRACT

In real-world IoT applications, sensor data is usually collected under diverse and dynamic contextual conditions where factors such as sensor placements or ambient environments can significantly affect data patterns and downstream performance. Traditional domain adaptation or generalization methods often ignore such context information or use simplistic integration strategies, making them ineffective in handling unseen context shifts after deployment. In this paper, we propose Chorus, a context-aware, data-free model customization approach that adapts models to unseen deployment conditions without requiring target-domain data. The key idea is to learn effective context representations that capture their influence on sensor data patterns and to adaptively integrate them based on the degree of context shift. Specifically, Chorus first performs unsupervised cross-modal reconstruction between unlabeled sensor data and language-based context embeddings, while regularizing the context embedding space to learn robust, generalizable context representations. Then, it trains a lightweight gated head on limited labeled samples to dynamically balance sensor and context contributions—favoring context when sensor evidence is ambiguous and vice versa. To further reduce inference latency, Chorus employs a context-caching mechanism that reuses cached context representations and updates only upon detected context shifts. Experiments on IMU, speech, and WiFi sensing tasks under diverse context shifts show that Chorus outperforms state-of-the-art baselines by up to 11.3% in unseen contexts, while maintaining comparable latency on smartphone and edge devices¹.

1 INTRODUCTION

Many Internet of Things (IoT) applications require integrating sensors such as mmWave radar, IMU and microphones that perceive the physical world for downstream analysis or control tasks [22]. However, these sensors usually operate under rapidly changing *contexts*, where operational and environmental conditions cause significant shifts in data distributions [11]. In wearable sensing, for instance, sensor placement encodes critical contextual information; an accelerometer trace differs markedly when a smartwatch is

*Corresponding author

¹The source code for Chorus will be released once the paper is accepted.

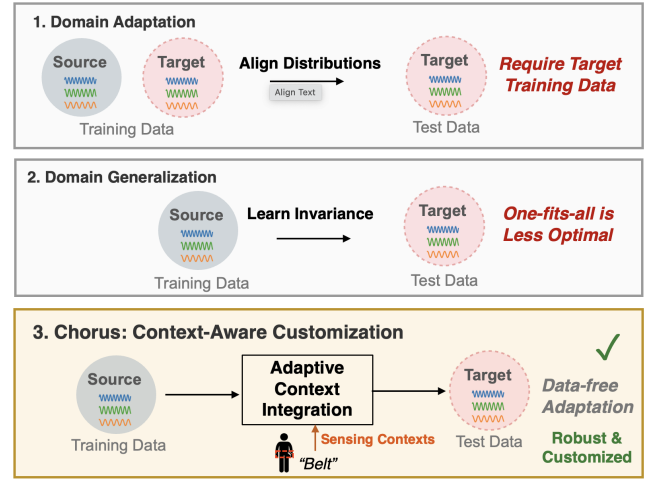


Figure 1: Chorus adaptively integrates context information into sensing models for data-free model customization, which outperforms existing domain adaptation and generalization approaches.

worn on the wrist versus clipped to the arm [27]. Similarly, for wireless sensing, Wi-Fi Channel State Information (CSI) signals change dramatically with the physical environment, such as in line-of-sight versus through-wall scenarios [12]. In machine learning, such a physical *context shift* induces a statistical *domain gap*, where data distributions differ significantly across contexts [37]. In our running example, a model trained on IMU data from “wrist” and “right pocket” contexts fails when deployed on a new “belt” placement if no target data are available. As summarized in Figure 1, domain adaptation tries to align source and target distributions but assumes access to target data, while domain generalization learns a single invariant model from source data alone. By contrast, Chorus uses adaptive gating with deployment-time context descriptions (e.g., “belt”) to customize predictions for the target context without seeing any target-domain samples.

Traditional methods to address this issue, illustrated in the top two panels of Figure 1, include domain adaptation [30, 32] and domain generalization [29, 38]. Domain generalization approaches attempt to learn domain-invariant features from multiple source domains; however, by seeking a universal representation, they often discard context-specific details

that are crucial for optimal performance in a particular target domain [7, 34]. On the other hand, domain adaptation aims to transfer knowledge from a source to a target domain but typically requires representative unlabeled target data during the training phase, limiting its applicability to entirely unseen contexts [32]. Although some recent work has tried to integrate context information into sensing models, it relies on simplistic integration strategies when combining sensor and context data, typically treating context as a static feature or a rule-based condition [16]. However, this oversimplifies the complex interaction between signal patterns and environmental contexts, often leading to suboptimal adaptation, especially under different degrees of context shift.[39].

To address these challenges, we propose Chorus, a new framework for context-aware data-free model customization for IoT sensing applications that adapts models to unseen deployment conditions without requiring target-domain training data. The key idea, illustrated in the bottom panel of Figure 1, is to learn effective context representations that capture their influence on sensor data patterns and to adaptively integrate these contexts into the model via a lightweight gating mechanism based on the degree of context shift.

Specifically, Chorus employs a two-stage training to achieve the goal with unlabeled data and a small amount of labeled data. First, Chorus trains sensor and context encoders via cross-modal reconstruction where the model learns to reconstruct sensor data from its corresponding context description, and vice versa. This process aligns the sensor and context representations in a shared latent space, enabling the encoder to capture how sensor patterns vary across different physical contexts. Moreover, we apply a regularization term that constrains and separates context embeddings in the latent space to improve the generalization ability to unseen contexts. Then in the second stage, Chorus freezes the encoders and trains only a lightweight classification head with limited labeled data. To balance the contributions of sensor and context information for downstream prediction, Chorus trains a lightweight gated head that generates ensemble weights of sensor and context embeddings according to the similarity between sensor and context embeddings and statistical distribution shifts. This can adaptively modulate the influence of sensor and context embeddings for each instance, favoring context when sensor evidence is ambiguous and vice versa. To further reduce inference latency, we introduce a context-caching mechanism that reuses cached context representations across consecutive samples and update the context cache when there are context shifts.

Our experimental evaluation on three public datasets under 16 diverse context conditions (including 5 IMU placements, 5 acoustic environments, and 6 WiFi deployments) demonstrates that Chorus improves accuracy in unseen contexts by up to 30% compared to domain-adversarial methods

and by 11.3% over the best context-aware baseline. Moreover, evaluations on mobile phones and NVIDIA edge devices show that Chorus incurs inference overhead equivalent to data-only approaches and lower than existing context-aware methods.

In summary, we make the following key contributions:

- We conduct an in-depth analysis of how context shifts affect performance of sensing applications, and show that simplistic context integration strategies are suboptimal in varying degrees of context shift.
- We propose Chorus, an adaptive context-aware framework that adapts models to unseen deployment conditions without requiring target-domain training data. Chorus extracts effective and generalizable context representations through regularized cross-modal reconstruction and trains an adaptive gating head to modulate the contributions of sensor and context embeddings across different context shifts.
- To further reduce inference latency, we introduce a context-caching mechanism that reuses cached context representations across consecutive samples and update the context cache when there are context shifts.
- Extensive evaluations on three different modalities across 16 contexts show that Chorus consistently outperforms state-of-the-art baselines particularly in challenging scenarios with large unseen domain gaps.

2 RELATED WORK

Domain Adaptation. Domain adaptation (DA) transfers knowledge from a labeled source domain to a distribution-shifted target domain, typically by aligning feature distributions [30, 32]. In IoT sensing, unsupervised DA has been applied to wearable HAR and multimodal mobile sensing using adversarial or contrastive objectives, such as ContrasGAN for cross-device HAR [21] and M3BAT for multimodal mobile sensing [15], as well as environment-independent device-free HAR and UniHAR-style cross-dataset deployment in MobiCom [9, 33]. A related line of work studies *model customization*, where a generic cloud or foundation model is further adapted to each device or application using additional data, for example PMC’s cloud-to-edge CNN customization based on device-specific statistics [13] or commercial foundation-model customization services [1]. Both DA and these customization frameworks, however, assume access to target-domain samples during training, whereas Chorus focuses on data-free customization for *unseen* deployment contexts.

Domain Generalization. Domain generalization (DG) aims to build models that are robust to unseen domains without using target data, often by enforcing domain-invariant

representations [38]. Representative approaches include adversarial schemes such as DANN [5] and multimodal variational autoencoders like JMVAE or MMVAE, which learn a shared latent space via cross-modal reconstruction [24, 26]. Benchmarks show that aggressively removing domain information can discard useful context-specific cues and yield limited gains under strong shifts [4, 7], and many generative models target high-level media or are too heavy for mobile sensing [18]. Recent DG methods for sensing (e.g., AFFAR, DGSense, SCAGOT [3, 19, 39]) improve robustness via branch fusion or episodic training, and SenSys’ FM-Fi cross-modal RF HAR system further demonstrates domain-generalized RF sensing [31], but still operate on a single sensor stream without explicit context embeddings, in contrast to Chorus’s context-aware encoder and adaptive head.

Context-aware Learning. Context-aware learning exploits side information such as locations, or environments to improve robustness. For example, fusing physiological signals with patient activity and location can reduce false alarms in clinical monitoring [11, 16], incorporating environmental context improves in-home patient monitoring [2], and early mobile continuous-sensing systems such as Jigsaw and DeepSense demonstrate how to manage rich context on smartphones [8, 14]. These systems demonstrate the value of context but typically rely on fixed fusion rules and do not decide *how strongly* to integrate context under different shift levels, and they usually assume access to deployment data. By contrast, Chorus explicitly encodes context into a regularized latent space and uses a gating controller to dynamically adjust the contribution of sensor and context features, enabling context-aware customization even when the target context is unseen during training.

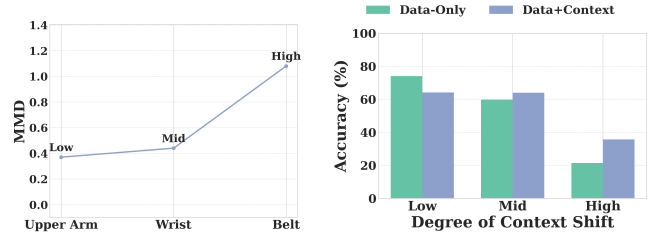
3 A MOTIVATION STUDY

In this section, we evaluate the performance of deep learning models for sensing applications under various context shifts and study the impact of incorporating context information on model accuracy.

3.1 Performance under Context Shifts

A key challenge for deep learning-based sensing applications is the performance degradation caused by shifts between training and testing contexts. In this section, we evaluate the performance of models trained with supervised learning under varying degrees of context shift.

Specifically, we evaluate model performance using IMU data from 10 subjects in the public Shoaib dataset [25] for human activity recognition (HAR). The task is to classify six human activities using wearable IMU sensor data, where the *context* is defined by different on-body sensor placements



(a) Degree of context shifts (b) Data-only vs. Data+Context measured by MMD.

Figure 2: Performance under varying context shifts and integration strategies.

of the wearables (e.g., wrist, pocket, belt, arm). To systematically analyze performance under varying context shifts, we quantify the degree of context shift between training and testing data using the Maximum Mean Discrepancy (MMD) metric [6], which measures the divergence between their feature distributions. A higher MMD score indicates a larger distributional gap and thus a greater context shift.

We use “Left pocket” and “Right pocket” as the source contexts for training data and compute MMD scores from this source distribution to all other placement locations. Based on these scores, we categorize three levels of context shift: *low* (“Upper arm”, MMD ≈ 0.37), *medium* (“Wrist”, MMD ≈ 0.44), and *high* (“Belt”, MMD ≈ 1.08). Figure 2a visualizes both the MMD values and the resulting accuracy drops of a supervised model when moving from the source pockets to these target contexts. As the MMD increases from the low-shift Upper arm to the high-shift Belt placement, the accuracy drop grows dramatically, indicating that sensing model performance is highly sensitive to the degree of *context shift*.

3.2 Impact of Context Integration

To address the performance degradation caused by context shifts, we further explore the integration of sensing context and evaluate its impact under varying degrees of shift.

Specifically, we compare two training strategies: a *Data-Only* approach that predicts solely from sensor data, and a *Data+Context* approach that concatenates sensor embeddings with context embeddings for classification. Here, context embeddings are derived using a pre-trained MiniLM-v2 sentence encoder applied to language-based placement descriptions such as “Upper arm” or “Left pocket”.

Figure 2b shows the performance of the two methods across different context shifts. The results reveal that naively injecting context through simple concatenation does not uniformly improve accuracy. For example, in the *Wrist* context (a mid shift), adding context improves accuracy from 59.8% (Data-Only) to 64.0%. In the high-shift *Belt* context, the improvement is more pronounced, rising from 21.4% to

35.7%. However, in the low-shift *Upper Arm* context, adding context reduces accuracy from 74.0% to 64.2%. These results demonstrate that a fixed integration strategy is unreliable, as performance depends heavily on the *degree of context shift*. This motivates the design where context representations are modulated adaptively at runtime based on the estimated degree of shift.

3.3 Summary

Our motivation study highlights two key insights that motivate the design of Chorus:

- The performance of sensing models degrades significantly as the degree of context shift between training and deployment increases, and this degradation correlates closely with the MMD-based shift metric.
- While incorporating context can be beneficial, a fixed integration strategy may harm performance in certain scenarios. The optimal balance between sensor and context information depends on the specific degree of *context shift*, highlighting the need for a dynamic, adaptive integration mechanism.

4 SYSTEM OVERVIEW

4.1 Applications and Challenges

Chorus is designed for a wide range of IoT sensing applications where sensor data is collected under diverse and dynamic contextual conditions. We define *context* as a set of environmental and operational factors—such as device placement, ambient noise, or user mobility—that systematically affect sensor data patterns. This contextual variability introduces a major challenge: models trained in one context often fail to generalize to others especially when no target-domain data is available prior to deployment. To address this, Chorus explicitly integrates context and models it as a learnable signal, enabling efficient, data-free model customization across unseen conditions.

We now describe several representative application scenarios, as illustrated in Figure 3. First, in human activity recognition with wearables, on-body sensor placement (e.g., wrist vs. ankle) is a critical context that drastically affects IMU signal patterns. For the same activity like “walking”, accelerometer and gyroscope readings exhibit different statistical properties depending on location. Second, in speech enhancement, environmental context, such as a quiet office versus bustling street, introduces varying ambient noise patterns in raw audio waveforms, complicating model adaptation in changing environments. Third, in wireless sensing, user mobility (stationary vs. moving) and physical environment (indoor vs. outdoor) significantly affect Wi-Fi Channel State Information (CSI) signals. These contexts introduce multipath fading

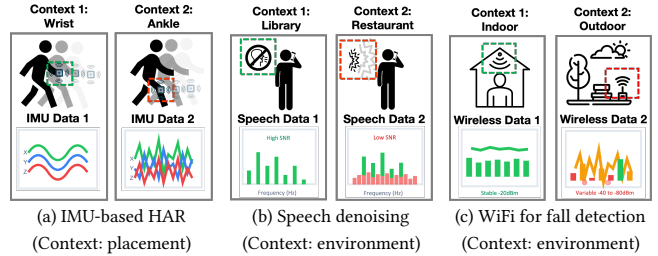


Figure 3: Context shifts in different sensing applications.

and Doppler shifts that significantly change the amplitude and phase characteristics of the signal.

Across these applications, contextual variation raises several technical challenges. First, the model should be able to generalize to unseen contexts, as collecting and annotating sufficient data for every possible context is impractical. Second, the relationship between context and the sensor data shifts is usually complex and task-dependent, requiring effective context representations and adaptive integration strategies. Moreover, many IoT sensing applications such as fall detection are time-critical, which requires a lightweight adaptation mechanism to reduce the inference latency.

4.2 Problem Formulation

The goal of Chorus is to enable data-free context-aware model customization for unseen contexts. The model is trained exclusively on data from source contexts and then deployed directly in target contexts where no data is available during training. Moreover, in many IoT sensing applications, collecting labeled data for every possible context is impractical, while basic context information (e.g., placement, room type, or device configuration) is often easy to log or infer from metadata and simple user input. Therefore, we aim to leverage abundant unlabeled data (sensor–context pairs) and a small amount of labeled data (sensor signals, context descriptions, and task labels) from source contexts to learn effective context representations and their impact on sensor data patterns.

4.3 System Architecture

The design of Chorus is motivated by the key insight from Section 3 that simplistic context integration is not robust enough to all scenarios. Therefore, our key idea is to learn effective context representations that capture their influence on sensor data patterns and to adaptively integrate these contexts into the model based on the degree of context shift. Figure 4 shows the overall system architecture.

We first extract effective and generalizable context representations from large-scale unlabeled *source* sensor–context pairs collected under diverse conditions. The context descriptions (e.g., environmental metadata or language-based

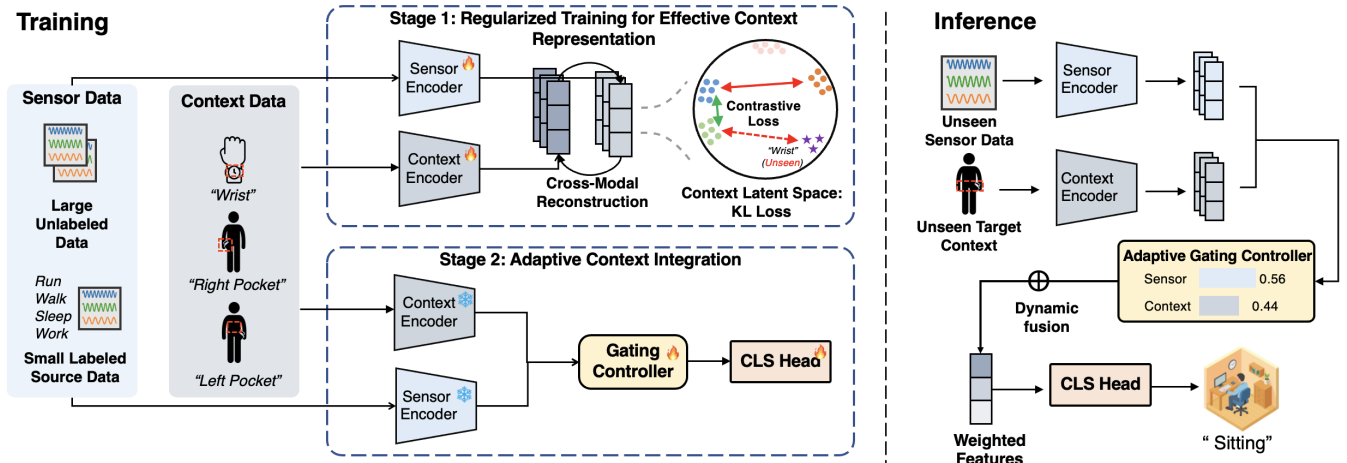


Figure 4: Chorus employs regularized cross-modal reconstruction on unlabeled sensor–context pairs to learn effective context representations, and integrates a lightweight gated head that adaptively integrates context features for prediction under varying degrees of unseen context shifts.

placement descriptions) are expressed in language format and input to feature encoders to extract context embeddings. Chorus trains sensor and context encoders via cross-modal reconstruction where the model learns to reconstruct sensor data from its corresponding context description, and vice versa. This process aligns the sensor and context representations in a shared latent space, enabling the encoder to capture how sensor patterns vary across different physical contexts such as on-body placement or noise type. Moreover, we further apply a regularization term that constrains and separates context embeddings in the latent space to improve the generalization ability to unseen contexts. In the second stage, Chorus employs a lightweight supervised customization strategy, where the pre-trained sensor encoder is frozen as a feature extractor, and only a small gated head is trained on limited labeled source data. Specifically, it incorporates an adaptive gating module that dynamically balances the contribution of sensor and context embeddings. Unlike fixed fusion methods (e.g., concatenation), our gating controller determines the fusion weights of the two embeddings at runtime based on two features: (i) alignment features from the cosine similarity between sensor and context embeddings, and (ii) dynamic features from simple statistics of the current sensor segment. This design enables the model to learn an adaptive strategy favoring context when the sensor pattern is ambiguous and prioritizing sensor data when shifts are mild. Since only the gating head is very lightweight, Chorus incurs minimal computational overhead. To further reduce runtime inference latency, Chorus employs a dynamic context cache mechanism that reuses cached context embeddings across consecutive samples and updates the cache only when a context shift is detected.

5 DESIGN OF CHORUS

Chorus first extracts effective and generalizable context representations through regularized cross-modal reconstruction, and then employs a lightweight gating module to adaptively integrate context information according to different context shifts. Chorus also features a dynamic context caching mechanism to further reduce inference latency.

5.1 Extracting Effective and Generalizable Context Representations

In the first stage of Chorus, we aim to train a context-aware sensor encoder f_{sensor} and context encoder $f_{context}$ using unlabeled sensor–context pairs to obtain a feature space that is explicitly sensitive to contextual factors. Suppose (x_s, c_s) denotes unlabeled sensor-context pairs in training data, where x_s denotes a masked sensor segment and c_s its associated, language-based context description. For example, in HAR, this context can be an on-body placement such as “Left pocket”, “Wrist”, or “Belt”, while in speech enhancement it can be an acoustic environment such as “Kitchen”, “Bus”, or “Office”. We first use a sensor and context encoder to map these inputs into a latent space, respectively:

$$z_x = f_{sensor}(x_s), \quad z_c = f_{context}(c_s).$$

Here the sensor encoder f_{sensor} is a modality-specific network (e.g., a 1D CNN backbone for IMU signals or a Transformer encoder for speech and WiFi features), and the context encoder $f_{context}$ is a lightweight text encoder (e.g., a pre-trained MiniLM-L12 sentence encoder) that embeds short context descriptions such as placement or environment names into a shared latent space.

5.1.1 *Cross-modal reconstruction.* We first try to map sensor and context embeddings into a shared latent space, so that we can capture alignment between context shifts and sensor pattern variation. Specifically, we propose to conduct bidirectional cross-modal reconstruction that minimizes the error of predicting one modality from the other (Figure 5):

$$\begin{aligned}\mathcal{L}_{x \rightarrow c} &= \text{MSE}(\hat{c}_s, c_s) = \text{MSE}(\text{Decoder}_c(z_x), c_s), \\ \mathcal{L}_{c \rightarrow x} &= \text{MSE}(\hat{x}_s, x_s) = \text{MSE}(\text{Decoder}_x(z_c), x_s).\end{aligned}$$

And the overall cross-modal reconstruction loss is calculated as:

$$\mathcal{L}_{\text{recon}} = \lambda_{x \rightarrow c} \mathcal{L}_{x \rightarrow c} + \lambda_{c \rightarrow x} \mathcal{L}_{c \rightarrow x}.$$

Here $\lambda_{x \rightarrow c}$ and $\lambda_{c \rightarrow x}$ control the relative importance of reconstructing context from sensor versus reconstructing sensor from context. In practice we set them to comparable values (e.g., both 1.0) so that neither direction dominates training, but they can be adjusted if one reconstruction is known to be noisier or less reliable.

Such cross-reconstruction objectives are widely used in multimodal generative models to align modalities in a shared latent space [24, 26, 35], where each encoder–decoder pair is forced to regenerate the other modality from a common representation. In our setting, this encourages the latent space to jointly capture (i) task-relevant structure (e.g., the underlying movement pattern of a walking activity) and (ii) systematic sensor pattern distortions induced by context (e.g., how that pattern is expressed on the ‘wrist’ versus the ‘ankle’). As a result, the sensor embeddings z_x become explicitly informative about context, providing a natural substrate for the downstream gated head to modulate the influence of sensor and context information, while the context embeddings z_c form compact, well-structured representations for each placement or environment that can be cached and reused at inference time.

5.1.2 *Latent regularization for context embeddings.* To improve the generalization ability to unseen contexts, we further regularize the context representations so that they focus on a subspace of context semantics rather than general language embeddings. Specifically, we add a lightweight regularization on the context embeddings:

$$\mathcal{L}_{\text{reg}} = \lambda(\mathcal{L}_{\text{KL}} + \gamma \mathcal{L}_{\text{con}}),$$

where \mathcal{L}_{KL} is the expected Kullback–Leibler divergence between the approximate posterior $q(z_c | c_s)$ and a standard Gaussian prior, and \mathcal{L}_{con} is a supervised contrastive loss that uses context labels to pull positives together and push negatives apart. The KL term \mathcal{L}_{KL} pulls the context posterior toward a standard Gaussian prior, keeping context embeddings in a compact space for descriptions of contexts rather than general language embeddings. The contrastive term \mathcal{L}_{con} is a supervised contrastive loss over context labels that

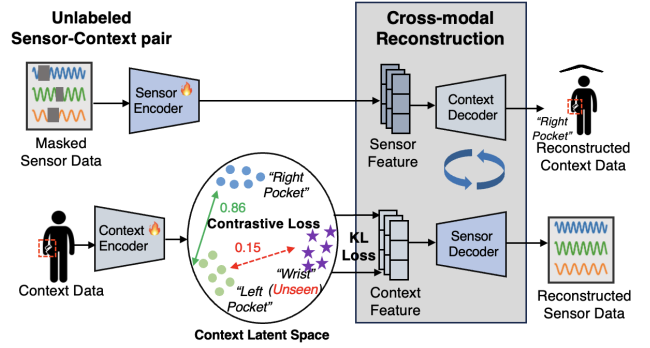


Figure 5: Learning effective context representations through cross-modal reconstruction and embedding space regularization.

pulls embeddings from the same context together and pushes different contexts apart, by treating samples with identical context IDs as positives and all others in the mini-batch as negatives. Together, these two terms avoid both unbounded drift and trivial collapse and produce clean, well-separated context embeddings that provide a stable control signal for the gating controller. In combination with the cross-modal reconstruction objective $\mathcal{L}_{\text{recon}}$ and the C_m -driven regularization schedule, this turns the context encoder into a dedicated, shift-aware module that carves out a compact, task-specific subspace from a generic language model.

Here we have two hyper-parameters λ and γ . Rather than tuning them separately for different datasets or applications, we determine them based on a context shift severity metric C_m derived from a sensor-only baseline. Specifically, C_m measures how much a sensor-only model degrades when moving from a Low-shift to a High-shift scenario for modality m : a small C_m indicates that the modality is relatively insensitive to context changes, whereas a large C_m means that performance is highly sensitive to context. We therefore map small, medium, and large values of C_m to weak, medium, and strong regularization regimes, respectively. The calculation of C_m and the resulting modality-wise assignments are described in Section 6.

Finally, the overall loss function for the first stage is:

$$\mathcal{L}_{\text{pre}} = \mathcal{L}_{\text{recon}} + \mathcal{L}_{\text{reg}}.$$

As a result, the pre-trained f_{sensor} serves as a context-aware feature extractor whose embeddings encode both task structure and context-induced distortions, while the pre-trained f_{context} produces compact, well-separated context representations that can be directly consumed and cached by the adaptive gating head in the second stage.

5.2 Adaptive Gating for Context Integration

In the second stage, Chorus employs a lightweight adaptive gating head that performs task-specific customization with

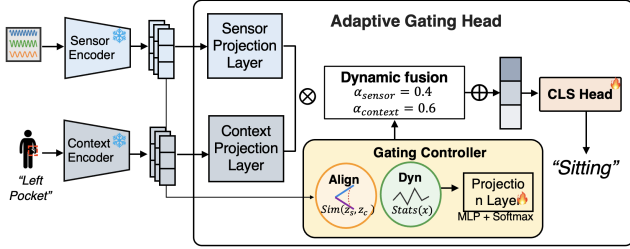


Figure 6: Adaptive context integration with a light-weight gating controller.

limited labeled data from source contexts. Chorus loads the pretrained model weights of the sensor and context encoders from the first stage, and freezes them. Given a small labeled source dataset $\mathcal{D}_{s,l}$, this head learns to balance the contributions of sensor and context information for different context shifts, so that the model can favor context when sensor evidence is ambiguous and rely more heavily on sensor data when the signal is clear.

5.2.1 Adaptive Gating Controller. To effectively capture different aspects of sensor data and context information, the head employs sensor and context projection layers, as shown in Figure 6. To dynamically blend the outputs of the two branches based on the specific context shifts, we introduce a lightweight *Gating Controller* (g_c), which is a small gating network mapping input features to routing weights over multiple experts (here, the sensor and context branches) [10, 23].

The controller’s decision is guided by a compact set of features, including: (i) alignment features derived from the cosine similarity between the sensor and context embeddings (how well they agree for the current sample), and (ii) dynamics features based on simple statistics of the input segment (e.g., norms and variances capturing local signal dynamics). These features are concatenated into $r(x)$ and fed to g_c . As these signals are computed for every sample, the same controller can react differently to different inputs. When the alignment between sensor and context embeddings is low and the local dynamics are unstable (Scenario A in Figure 6), the gate increases α_{context} and relies more on contextual cues; when alignment is high and dynamics are stable (Scenario B), it increases α_{sensor} and relies more on the sensor data.

Given a gating feature vector $r(x)$ extracted from the current input, the controller applies a small MLP and produces logits over the two branches, which are converted via a softmax into weights

$$\alpha(x) = [\alpha_{\text{sensor}}(x), \alpha_{\text{context}}(x)] = \text{softmax}(g_c(r(x))) \in \mathbb{R}^2.$$

In this way, the gating controller implements instance-wise adaptation to changing contexts instead of using a fixed fusion rule.

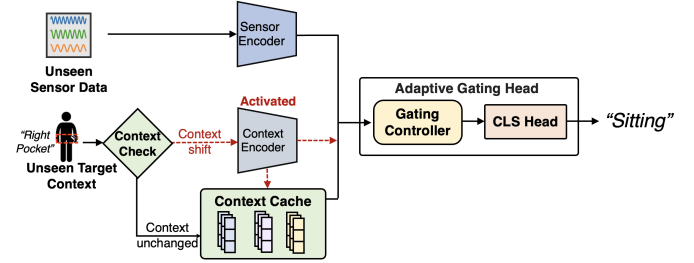


Figure 7: Dynamic context caching during inference.

The final representation h_{final} is obtained via a weighted sum of the two branch outputs:

$$h_{\text{final}} = \alpha_{\text{sensor}} h_{\text{sensor}} + \alpha_{\text{context}} h_{\text{context}}.$$

This allows the model to dynamically increase α_{context} when the sensor features are ambiguous or strongly shifted, and to focus on α_{sensor} when the patterns are stable, mirroring the high-level behavior described in the abstract. A final classifier operates on h_{final} to produce the prediction \hat{y} .

5.2.2 Training objective for the gating head. To encourage the gate to genuinely trade off sensor and context information rather than collapsing to a single branch, we add a simple load-balancing term on top of the standard classification loss. We optimize a combined loss function for this stage:

$$\mathcal{L}_{\text{custom}} = \mathcal{L}_{\text{CE}}(y, \hat{y}) + \lambda_{\text{balance}} \mathcal{L}_{\text{balance}},$$

where \mathcal{L}_{CE} is the standard cross-entropy loss, and $\mathcal{L}_{\text{balance}}$ is a load balancing regularization term. This regularization avoids degeneration of the gating mechanism into a trivial solution where it exclusively relies on a single branch (e.g., ignoring context entirely), leading to expert collapse [23]. To prevent this, $\mathcal{L}_{\text{balance}}$ penalizes the deviation of the average gating weights across a batch from a uniform distribution (i.e., target usage of $1/K$ for K branches). The scalar λ_{balance} controls the strength of this regularization, ensuring that the model learns to effectively leverage both sensor-intrinsic patterns and contextual cues for generalization.

5.3 Dynamic Context Caching

To mitigate the computational overhead of repeatedly encoding context features, we exploit the high temporal locality inherent in real-world streaming scenarios. In typical IoT deployments, contextual descriptors and their resulting embeddings often remain stable across extended sequences of input samples. For example, device placement does not change within a session, acoustic environments persist for minutes, and wireless environments evolve much more slowly than packet-level traffic. Therefore, rather than recomputing the context embedding for every sample during inference, Chorus maintains a small cache that stores the processed latent representation z_{context} for the current context.

During inference, each incoming sample is accompanied by a context identifier (e.g., a placement label or environment tag). The system first checks whether this identifier matches the one used for the previous sample. If the identifier is unchanged, Chorus simply looks up the cached z_{context} and feeds it to the adaptive head without invoking the context encoder. If the identifier differs, indicating a genuine context shift, the context description is passed through the text encoder and projection layers to produce a new latent representation, which is then inserted into the cache and used for fusion. In streaming workloads, where context changes are much rarer than new sensor samples, this simple protocol achieves high cache hit rates and substantially reduces the number of expensive context-encoding operations.

The cache stores the output of the full context-processing stack, after adaptation and normalization, so that all subsequent steps reuse the same control features. This effectively turns context encoding from a per-sample operation into an occasional update triggered only when a context shift occurs, reducing both latency and energy consumption on resource-constrained edge devices.

6 EVALUATION

We evaluate how well Chorus achieves context-aware, data-free model customization across sensing modalities, degrees of context shift, and hardware platforms, and analyze the contribution of each design component.

6.1 Methodology

6.1.1 Datasets. We use three public datasets covering inertial sensing, speech, and WiFi signals (Table 1). For Shoaib, we use tri-axial IMU streams from 10 users with five on-body locations (Belt, Left/Right pocket, Upper arm, Wrist) as contexts. For VoiceBank-DEMAND, we follow the standard 28/2 speaker split and treat DEMAND noise types as acoustic contexts. For CSI-Bench, we use the FallDetection subset with six environments as contexts. We adopt common preprocessing for each modality (sliding windows for IMU, STFT-based time–frequency features for speech, fixed-length CSI sequences for WiFi).

6.1.2 Experimental Settings. To study robustness under controlled context shifts, we construct Low/Mid/High tiers using an MMD-based distance between fixed source contexts and unseen target contexts (Table 2). For each modality, we choose two source contexts for training and one held-out target context in each tier for testing. We pre-train the context-aware encoder on 80% unlabeled sensor–context pairs from the source contexts, and train the adaptive head using 1–10% labeled source data on the same contexts. This scenario-level tiering is separate from the modality-level shift index C_m in §3.1, which is only used to choose the strength of latent

Dataset	Modality	Task	Context (#)	# of subjects
Shoaib [25]	IMU	HAR	Placement (5)	10
VoiceBank-DEMAND [28]	Speech	Denosing	Environment (10)	30
CSI-Bench [40]	WiFi	Fall Detection	Environment (6)	17

Table 1: Summary of datasets used in the evaluation.

Modality	Source contexts	Target	Shift	MMD
IMU	left/right pocket	upper arm	Low	0.365
		wrist	Mid	0.442
		belt	High	1.081
WiFi	large house, office	medium house	Low	0.227
		apartment	Mid	0.263
		villa	High	0.356
Speech	kitchen, restaurant	living room	Low	0.059
		office	Mid	0.120
		bus	High	0.166

Table 2: Settings of context shifts for different datasets. The degree of shift (Low/Mid/High) is defined by MMD scores between source (train) and unseen target (test) contexts.

regularization during pre-training. Unless otherwise noted, all methods follow a strict source-only protocol without access to any target-domain data and are evaluated directly on unseen target contexts.

6.1.3 Baselines. To isolate the effect of context handling, all methods for a given modality (including Chorus) share the same backbone architecture. We compare Chorus against the following baselines:

- **Sensor-Only.** Backbone trained only on sensor inputs from labeled source data, ignoring context.
- **Fix-Add.** Fixed fusion by element-wise addition of sensor and context features before the classifier.
- **Fix-Concat.** Fixed fusion by concatenating sensor and context features before the classifier.
- **Fix-Attn.** Single cross-attention layer attending from sensor to context features with shared parameters.
- **SupCon.** Supervised contrastive learning on fused sensor+context embeddings, followed by a frozen encoder and classifier.
- **TS-TST.** Self-supervised pre-train then fine-tune baseline using TS-TST [36].
- **DANN.** Domain-Adversarial Neural Networks [5] with a gradient-reversal layer and domain classifier.
- **M3BAT.** Multi-branch adversarial training with separate discriminators for different feature groups [15].
- **ContrasGAN.** DANN-style adversarial loss plus a contrastive objective on latent features [21].

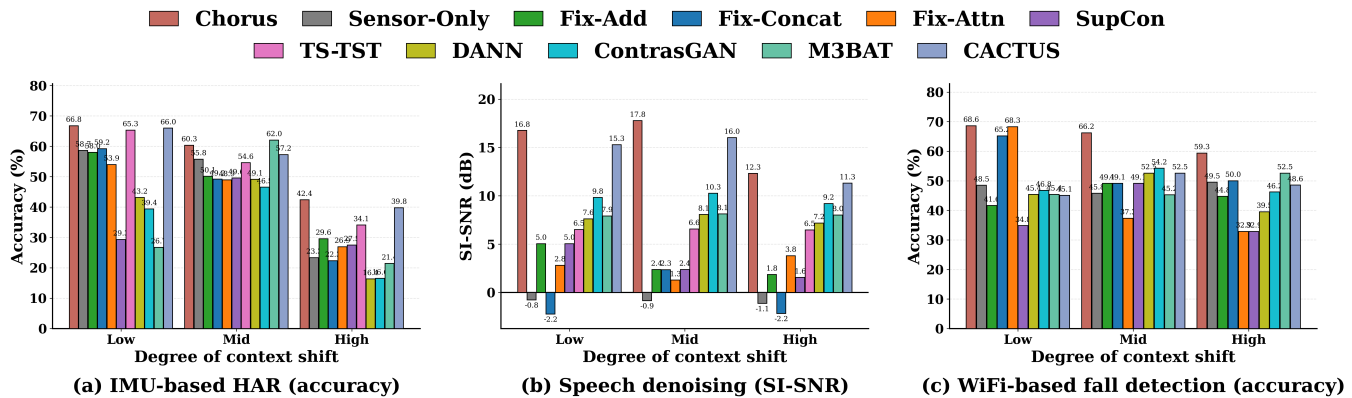


Figure 8: Performance across degrees of context shifts for IMU-based human activity recognition (HAR), speech denoising, and WiFi-based fall detection.

- **CACTUS**. Context-specialization baseline with multiple lightweight μ -classifiers selected by context labels [20].

Some baselines (e.g., DANN, ContrasGAN, M3BAT) assume additional unlabeled target data, whereas Chorus uses only source-domain sensor–context pairs and adaptive gating.

6.1.4 Configurations. Within each modality, we use a compact 1D CNN backbone for IMU HAR and a Transformer encoder for speech denoising and WiFi fall detection, with shared hidden dimensions and depth across methods.² All models are trained with AdamW for up to 100 epochs with early stopping on validation loss, and we report accuracy, F1, precision, and recall for IMU/WiFi and SI-SNR for speech. The context-aware encoder is pre-trained with the reconstruction and regularization objective in §5.1 under three regimes along a regularization axis: (i) weak regularization with $\lambda \approx 0$ (reconstruction-dominated), (ii) KL-only regularization with $\lambda > 0, \gamma = 0$, and (iii) strong regularization with both KL and contrastive terms active ($\lambda > 0, \gamma > 0$). Instead of tuning (λ, γ) separately for every experiment, we assign one regime per *modality* m (IMU, WiFi, Speech) using a simple shift–severity index $C_m = 1 - \text{Perf}_{\text{High}}/\text{Perf}_{\text{Low}}$ computed from the sensor-only backbone in Table 2. Empirically, $C_{\text{WiFi}} \approx 0.19$, $C_{\text{IMU}} \approx 0.37$, and $C_{\text{Speech}} \approx 0.48$, which we interpret as weak, medium, and strong shift severity and map to weak, medium, and strong context regularization, respectively. These modality-wise choices are fixed across all experiments and remove the need for per-setting hyperparameter search.

6.1.5 Implementation. We deploy Chorus on two edge platforms to evaluate cross-platform scalability. For speech denoising, we use an NVIDIA Jetson Orin Nano [17] with a GPU-accelerated PyTorch backend; for IMU HAR, we use

a Samsung smartphone running a Linux environment via Termux with a CPU-only PyTorch backend, representing a battery-constrained personal device. On both platforms, we export models as TorchScript for consistent and efficient inference. Audio features are extracted via a Short-Time Fourier Transform (STFT), and IMU streams are normalized with simple sensor-wise calibration to account for device-level variations.

6.2 Overall Performance

We now compare Chorus and all baselines across modalities and degrees of context shift under our source-only customization setting. We first fix the labeled source budget to 1% and vary the degree of context shift (Low/Mid/High) for IMU, speech, and WiFi (Figure 8), and then zoom in on the hardest IMU configuration (High-shift “Belt” target) to study how performance changes with more labeled source data and with a small amount of target labels (Figure 9).

6.2.1 Performance across different degrees of context shift. Guided by the MMD-based construction in §3 (Table 2), we fix the labeled source budget to 1% for all three modalities and vary only the degree of context shift, so that differences mainly reflect robustness to unseen deployment contexts. On IMU HAR (Figure 8a), Chorus reaches 66.8%, 60.3%, and 42.4% accuracy in the Low/Mid/High tiers, consistently surpassing strong context-aware and domain-adaptation baselines. On speech denoising (Figure 8b), Chorus achieves 16.8 dB, 17.8 dB, and 12.3 dB SI-SNR, about 1–2 dB above CACTUS in each tier while still delivering large gains over Sensor-Only and simple fusion baselines. For WiFi fall detection (Figure 8c), Chorus attains 68.6%, 66.2%, and 59.3% accuracy, again matching or exceeding the best competitor. Across modalities, generic domain-adversarial and contrastive methods (DANN, ContrasGAN, M3BAT, SupCon) can be competitive in the Low tier but quickly degrade towards chance

²TS-TST [36] is the only baseline that requires its own Transformer-based architecture.

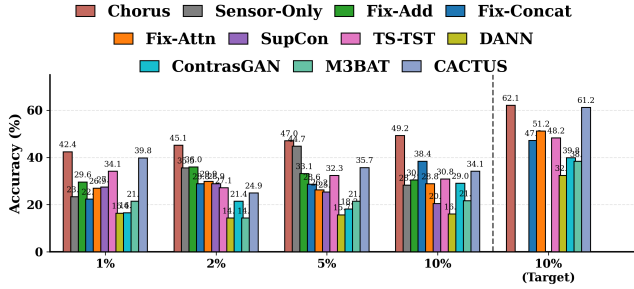
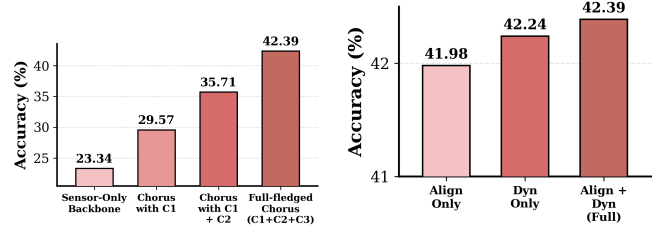


Figure 9: Performance with different amounts of labeled data and data from target domain.

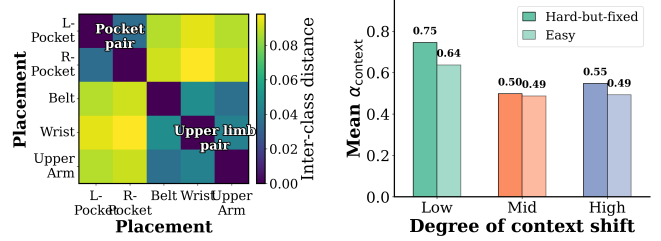
under High shift, sometimes even falling below Sensor-Only, whereas Chorus and CACTUS remain stable. Overall, Chorus enjoys a clear margin in the Mid/High tiers for IMU and WiFi and slightly outperforms CACTUS on speech, supporting our claim that explicit context-aware fusion provides a more robust inductive bias than fixed fusion or purely domain-invariant training under label scarcity.

6.2.2 Performance with different amounts of data. Figure 9(a) considers the hardest IMU scenario (High shift, “Belt” as unseen target) and varies the labeled *source-domain* budget from 1% to 10%, while keeping the unlabeled pre-training set fixed. Chorus improves steadily with more source labels, rising from 42.4% to 49.2% accuracy, whereas most baselines plateau in the low–mid 30% range; for example, CACTUS remains roughly 8–15 percentage points lower across the same budgets. Several domain-adversarial and contrastive methods (DANN, ContrasGAN, M3BAT, SupCon) hover near the 7-class chance level (about 14.3%) even as more labeled source data are added, suggesting that aggressively enforcing invariance on source contexts can suppress discriminative placement information before a reliable classifier is learned. Thus, increasing labeled source data helps only when paired with an adaptive, context-aware gating policy, rather than with unstable domain-alignment objectives.

6.2.3 Performance with a limited amount of target-domain data. We further examine how Chorus behaves when a small amount of labeled target data is available and run a Belt-only adaptation experiment on the same IMU configuration (High shift with “Belt” as the target domain). The encoder is pre-trained on 80% unlabeled sensor–context pairs from the source domains (Left/Right pocket), and we then fine-tune only the task head with 10% labeled Belt samples before evaluating on the Belt test set, updating only the adaptive head for Chorus and the last layer(s) for each baseline under the same target-label budget. Figure 9(b) shows that Chorus reaches 62.1% accuracy on Belt, slightly exceeding CACTUS (61.2%) and clearly outperforming the best fixed-fusion baseline TS-TST (48.2%), while domain-adversarial and generative baselines remain much lower (e.g., ContrasGAN 39.8%, M3BAT



(a) Design modules. (b) Different gating signals. Figure 10: Ablation study.



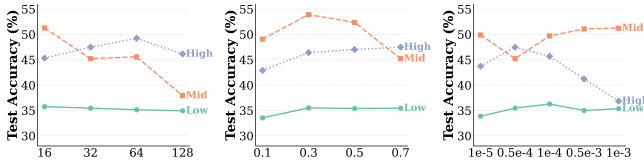
(a) Distance of different context embeddings. (b) Context weights generated by the gating controller. Figure 11: Intermediate results.

38.3%, DANN 32.3%). Even with limited target supervision, simply aligning feature distributions is therefore insufficient; explicitly modeling deployment context and adapting sensor–context fusion remains crucial for robust performance.

6.3 Understanding Chorus’s performance

We now perform an ablation study to understand what Chorus actually learns and how each component contributes to robustness under context shifts.

6.3.1 Ablation study. Figure 10a compares the mean accuracy with different design components of Chorus on the hardest IMU scenario (1% labels, High shift). We gradually add three components: C1 augments the sensor backbone with context features using static fusion, C2 introduces an adaptive gating controller to reweight sensor and context paths, and C3 initializes the encoder with VAE based context-aware pre-training. Starting from a Sensor-Only backbone (23.3% accuracy), adding C1 raises the accuracy to 29.6%, and further adding C2 increases it to 35.7%; with all three components enabled (full Chorus, C1+C2+C3), the accuracy reaches 42.4%, yielding a total gain of +19.1 percentage points. Figure 10b further evaluates the gating inputs Align and Dyn introduced in §5.2: an Align-only gate achieves 42.0% accuracy and a Dyn-only gate reaches 42.2%, while the full Align+Dyn variant attains 42.4%. Although the absolute differences are small in this hard regime, the monotonic improvements from C1–C3 and the consistent edge of Align+Dyn together validate the effectiveness of Chorus’s architectural design and gating signal choices.



(a) Batch size. (b) Dropout rate. (c) Learning rate.

Figure 12: Performance of Chorus with different hyperparameters.

6.3.2 Effectiveness of context representations. The learned context embeddings form clean and semantically meaningful clusters. A linear probe on frozen embeddings achieves 100% placement accuracy with a silhouette score of 1.0, indicating highly separated and compact classes. As shown in Figure 11(a), the two pockets (L-/R-pocket) lie close to each other yet far from belt and wrist, while wrist and upper-arm appear as a nearby upper-limb pair, matching their physical relationships and confirming that context codes provide a reliable control signal.

6.3.3 Outputs of the gating controller across different context shifts. The gating controller assigns higher context weight precisely where context is most useful. The Low and High scenarios, where Sensor-Only is weakest and Chorus yields the largest accuracy gains (cf. Figure 8), receive the highest mean α_{context} , while the Mid tier uses a more balanced fusion. Figure 11(b) further shows that, within each tier, hard-but-fixed samples (Sensor-Only wrong, Chorus correct) systematically get more context weight than easy samples; for example, in the Low tier the gate assigns higher α_{context} to hard-but-fixed samples than to easy ones. Together, these trends indicate that the controller has learned an intuitive policy: trust context more when sensor evidence is unreliable and fall back to sensor features when the signal is clear.

6.4 Micro-benchmark Performance

We next assess how sensitive Chorus is to basic training hyperparameters in the hardest IMU scenario (High shift, “Belt” target), by varying batch size, dropout, and learning rate and reporting accuracy across the Low/Mid/High context shift tiers.

6.4.1 Impact of batch sizes. In Figure 12a, accuracies in all three tiers stay within a narrow band when the batch size varies from 16 to 64, with only mild gains in the High tier. This indicates that Chorus is largely insensitive to batch size in the small-to-medium range. Very large batches bring no benefit and can hurt the Mid tier (e.g., batch 128), suggesting that standard sizes already sit in a stable region.

6.4.2 Impact of dropout rates. Figure 12b shows that all tiers perform best or near-best for moderate dropout around 0.3–0.5; for instance, the Mid tier peaks near 0.3 and the

Method	Params (M)	Size (MB)	Latency (ms)	Memory (MB)	Energy (mJ)
Sensor Only	2.26	8.62	648	703	1944
DANN	2.33	8.88	1286	716	3859
CACTUS	15.4	58.74	1465	750	4395
Chorus w/o Cache	2.33	8.88	712	1087	2135
Chorus	2.33	8.88	673	1087	2018

Table 3: Comparison of system overhead on Jetson Orin Nano for speech enhancement.

High tier remains strong up to 0.5. Extremely low (0.1) or high (0.7) dropout slightly reduces accuracy, but the overall curves remain flat, indicating that Chorus does not rely on fine-tuned dropout.

6.4.3 Impact of learning rates. Figure 12c shows a clear, but forgiving, trend with respect to the learning rate. All tiers achieve strong performance between 5×10^{-5} and 10^{-4} , with our default 10^{-4} lying near the center of this plateau. Moving outside this band degrades performance gradually rather than catastrophically—for example, very small steps (10^{-5}) slow progress and overly aggressive rates (5×10^{-4} or 10^{-3}) mainly hurt the High tier—showing that Chorus works well under standard optimizer settings.

6.5 System Overhead

Beyond adaptation accuracy, practical deployment also requires low computational overhead. We therefore evaluate inference latency, throughput, memory footprint, and energy consumption on two edge platforms: a Jetson Orin Nano for speech enhancement and a Samsung smartphone for IMU-based activity recognition. Compared to DANN, which adds a domain discriminator and requires domain labels during training, and CACTUS, which uses a dual-model architecture (7.67M “big model” + 7.73M “micro model” + context scorer, a $6.8\times$ parameter increase), Chorus only introduces a lightweight context encoder (67K parameters) and a small gating controller, achieving dynamic context-aware adaptation without auxiliary models or adversarial training.

6.5.1 Comparison of system overhead with baselines. Table 3 and Figure 13 summarize architectural complexity and runtime. Chorus achieves context-aware adaptation with 2.33M parameters (8.88 MB), adding only 3.0% parameters over the sensor backbone, whereas CACTUS requires 15.4M parameters ($6.6\times$ larger). With context caching, Chorus reaches latencies comparable to sensor-only baselines—673 ms for speech (3.9% overhead) and 9.45 ms for IMU—while DANN and CACTUS more than double speech latency. Energy consumption follows a similar trend: Chorus consumes 2018 mJ per speech sample, saving roughly half the energy compared to DANN and CACTUS.

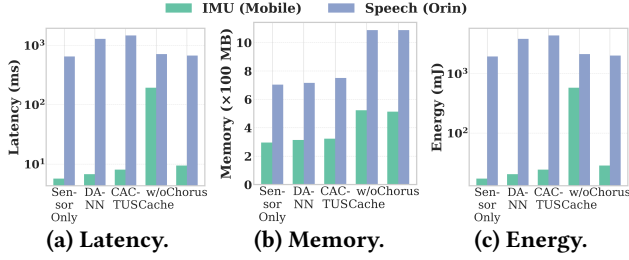


Figure 13: Impact of backbone complexity: IMU vs. Speech.

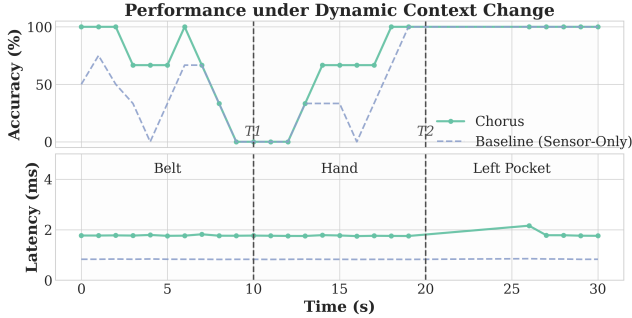


Figure 14: Accuracy (top) and inference latency (bottom) under dynamic context changes; T_1 and T_2 mark the time of context changes.

6.5.2 *Impact of backbone complexity.* The two platforms illustrate how overhead scales with backbone complexity. For speech, STFT/ISTFT preprocessing dominates runtime (96.3% of inference time), so Chorus’s adaptation adds only about 4% overhead and caching provides modest gains. For IMU, the lightweight backbone (5.69 ms) makes the text encoder the main bottleneck: without caching, latency rises to 193 ms (33.9× increase), but caching reduces it to 9.45 ms (20.4× reduction), achieving 91.9 samples/second and comfortably meeting the 50 Hz real-time requirement. Overall, context caching is key for low-latency deployment across backbones, and Chorus stays within 9 MB of storage and under 550 MB peak memory.

6.5.3 *Performance under dynamic context changes.* We finally examine how Chorus behaves under dynamic context changes on a custom smartphone HAR demo. IMU data from seven subjects with Belt and Hand placements are used for pre-training and fine-tuning, and a held-out subject performs a 30 s sequence: standing at the belt, walking with the phone in hand, and walking with the phone in the left pocket (unseen). Figure 14 shows that Chorus maintains higher accuracy than the sensor-only baseline throughout the trace and adapts quickly after the two context switches at T_1 and T_2 , improving accuracy by roughly 10–20 percentage points on seen placements and reaching 75.8% vs. 62.1% over the full 30 s. This robustness comes with only a small runtime cost: after warm-up, Chorus runs at about 1.7–2.0 ms per

window compared to 0.8–0.9 ms for the baseline and stays below 2.2 ms even in the unseen stage, trading less than 1 ms additional latency for substantially more stable performance under dynamic context changes.

7 DISCUSSION

Estimating context information. Our current design requires integrate language descriptions of context information. In the future, we will explore how to infer latent context directly from raw multi-sensor streams or via weak/self-supervision, so that Chorus can retain context-aware, data-free customization even when explicit context annotations are sparse or noisy.

Generalize to multiple context shifts. In this paper, we evaluate Chorus across three sensing modalities under a major source of context shift, such as changes in sensor placement or environment. In the future, we will extend Chorus to handle multiple interacting context factors—for example, sensor patterns jointly influenced by hardware variations, subject differences, and long-term behavioral drift.

Integrating advanced training strategies and richer gating signals. In this paper, we freeze the sensor backbone and train the gating controller using limited labeled data. However, we observe that aggressively enforcing domain invariance in the backbone can be counterproductive under large context shifts, whereas explicitly leveraging structured context as a control signal proves beneficial. Moreover, the current design relies on a small set of hand-crafted signals. In future work, we aim to explore richer gating signals and carefully constrained backbone updates, enabling the gate and backbone to co-adapt without compromising backbone stability.

8 CONCLUSION

In this paper, we introduce Chorus, a context-aware, data-free customization approach that adapts models to unseen deployment conditions without requiring target-domain data. Chorus learns robust context representations through regularized cross-modal reconstruction, and integrates them via a lightweight gating controller that dynamically adjusts to varying degrees of context shift. To reduce inference latency, it employs a context-caching mechanism that reuses cached representations and updates only when a context change is detected. Experiments on IMU, speech, and WiFi sensing tasks under diverse context shifts show that Chorus outperforms state-of-the-art baselines in unseen contexts while maintaining comparable latency on smartphones and edge devices. In the future, we will extend Chorus to more general scenarios, including estimating context information, handling multiple simultaneous context shifts, and incorporating richer gating signals.

REFERENCES

- [1] [n. d.]. Customize your model to improve its performance for your use case. <https://docs.aws.amazon.com/bedrock/latest/userguide/custom-models.html>. ([n. d.]). Accessed: 2025-12-01.
- [2] Mattia Giovanni Campana and Franca Delmastro. 2021. COMPASS: Unsupervised and online clustering of complex human activities from smartphone sensors. *Expert Systems with Applications* 181 (2021), 115124. <https://doi.org/10.1016/j.eswa.2021.115124>
- [3] Furong Duan, Tao Zhu, Liming Chen, Huansheng Ning, Chao Liu, and Yaping Wan. 2025. SCAGOT: Semi-Supervised Disentangling Context and Activity Features Without Target Data for Sensor-Based HAR. *IEEE Sensors Journal* 25, 8 (April 2025), 14220–14234. <https://doi.org/10.1109/JSEN.2025.3543928>
- [4] Jean-Christophe Gagnon-Audet, Kartik Ahuja, Mohammad Javad Darvishi Bayazi, Pooneh Mousavi, Guillaume Dumas, and Irina Rish. 2023. WOODS: Benchmarks for Out-of-Distribution Generalization in Time Series. *Transactions on Machine Learning Research* (2023). <https://openreview.net/forum?id=mvftzofTYQ> Featured Certification.
- [5] Yaroslav Ganin, Evgeniya Ustinova, Hana Ajakan, Pascal Germain, Hugo Larochelle, François Laviolette, Mario Marchand, and Victor Lempitsky. 2016. Domain-adversarial training of neural networks. *The journal of machine learning research* 17, 1 (2016), 2096–2030.
- [6] Arthur Gretton, Karsten M. Borgwardt, Malte J. Rasch, Bernhard Schölkopf, and Alexander Smola. 2012. A Kernel Two-Sample Test. *Journal of Machine Learning Research* 13, Mar (2012), 723–773. <http://www.jmlr.org/papers/v13/gretton12a.html>
- [7] Ishaan Gulrajani and David Lopez-Paz. 2021. In Search of Lost Domain Generalization. In *International Conference on Learning Representations (ICLR)*. <https://openreview.net/forum?id=lQdXeXDoWtI>
- [8] Loc N. Huynh, Rajesh K. Balan, and Youngki Lee. 2016. DeepSense: A GPU-based Deep Convolutional Neural Network Framework on Commodity Mobile Devices. In *Proceedings of the 2016 Workshop on Wearable Systems and Applications (WearSys), co-located with MobiSys*. ACM, 25–30.
- [9] Wenjun Jiang, Chenglin Miao, Fenglong Ma, Shuochoao Yao, Yaqing Wang, Ye Yuan, Hongfei Xue, Chen Song, Xin Ma, Dimitrios Koutsonikolas, Wenyao Xu, and Lu Su. 2018. Towards Environment Independent Device Free Human Activity Recognition. In *Proceedings of the 24th Annual International Conference on Mobile Computing and Networking (MobiCom)*. ACM, 289–304. <https://doi.org/10.1145/3241539.3241555>
- [10] Michael I. Jordan and Robert A. Jacobs. 1994. Hierarchical Mixtures of Experts and the EM Algorithm. *Neural Computation* 6, 2 (1994), 181–214. <https://doi.org/10.1162/neco.1994.6.2.181>
- [11] Barbara T. Korel and Simon G. M. Koo. 2010. A Survey on Context-Aware Sensing for Body Sensor Networks. *Wireless Sensor Network* 2, 8 (2010), 571–583. <https://doi.org/10.4236/wsn.2010.28069>
- [12] Manikanta Kotaru, Kiran Joshi, Dinesh Bharadia, and Sachin Katti. 2015. SpotFi: Decimeter Level Localization Using WiFi. *SIGCOMM Comput. Commun. Rev.* 45, 4 (Aug. 2015), 269–282. <https://doi.org/10.1145/2829988.2787487>
- [13] Bingyan Liu, Yuanchun Li, Yunxin Liu, Yao Guo, and Xiangqun Chen. 2020. PMC: A Privacy-preserving Deep Learning Model Customization Framework for Edge Computing. *Proceedings of the ACM on Interactive, Mobile, Wearable and Ubiquitous Technologies* 4, 4 (2020), 139:1–139:25. <https://doi.org/10.1145/3432208>
- [14] Hong Lu, Jun Yang, Zhigang Liu, Nicholas D. Lane, Tanzeem Choudhury, and Andrew T. Campbell. 2010. The Jigsaw Continuous Sensing Engine for Mobile Phone Applications. In *Proceedings of the 8th ACM Conference on Embedded Networked Sensor Systems (SensSys)*. ACM, 71–84. <https://doi.org/10.1145/1869983.1869992>
- [15] Lakmal Meegahapola, Hamza Hassoune, and Daniel Gatica-Perez. 2024. M3BAT: Unsupervised Domain Adaptation for Multimodal Mobile Sensing with Multi-Branch Adversarial Training. *Proc. ACM Interact. Mob. Wearable Ubiquitous Technol.* 8, 2, Article 46 (May 2024), 30 pages. <https://doi.org/10.1145/3659591>
- [16] Fen Miao, Yayu Cheng, Yi He, Qingyun He, and Ye Li. 2015. A Wearable Context-Aware ECG Monitoring System Integrated with Built-in Kinematic Sensors of the Smartphone. *Sensors* 15, 5 (2015), 11465–11484. <https://doi.org/10.3390/s150511465>
- [17] NVIDIA Corporation. 2024. NVIDIA Jetson Orin. <https://www.nvidia.com/en-us/autonomous-machines/embedded-systems/jetson-orin/> (2024).
- [18] Heiko Oppel and Michael Munz. 2024. IMUDiffusion: A Diffusion Model for Multivariate Time Series Synthesis for Inertial Motion Capturing Systems. (2024). arXiv:cs.LG/2411.02954 <https://arxiv.org/abs/2411.02954>
- [19] Xin Qin, Jindong Wang, Yiqiang Chen, Wang Lu, and Xinlong Jiang. 2023. Domain Generalization for Activity Recognition via Adaptive Feature Fusion. *ACM Trans. Intell. Syst. Technol.* 14, 1 (2023), 9:1–9:21. <https://doi.org/10.1145/3552434>
- [20] Mohammad Mehdi Rastikerdar, Jin Huang, Shiwei Fang, Hui Guan, and Deepak Ganesan. 2024. CACTUS: Dynamically Switchable Context-aware Micro-Classifiers for Efficient IoT Inference. In *Proceedings of the 22nd Annual International Conference on Mobile Systems, Applications and Services (MobiSys '24)*. Association for Computing Machinery, New York, NY, USA, 505–518. <https://doi.org/10.1145/3643832.3661888>
- [21] Andrea Rosales Sanabria, Franco Zambonelli, Simon Dobson, and Juan Ye. 2021. ContrasGAN: Unsupervised domain adaptation in Human Activity Recognition via adversarial and contrastive learning. *Pervasive Mob. Comput.* 78, C (Dec. 2021), 18. <https://doi.org/10.1016/j.pmcj.2021.101477>
- [22] Mahadev Satyanarayanan. 2017. The Emergence of Edge Computing. *Computer* 50, 1 (2017), 30–39. <https://doi.org/10.1109/MC.2017.9>
- [23] Noam Shazeer, Azalia Mirhoseini, Krzysztof Maziarz, Andy Davis, Quoc V. Le, Geoffrey E. Hinton, and Jeff Dean. 2017. Outrageously Large Neural Networks: The Sparsely-Gated Mixture-of-Experts Layer. In *5th International Conference on Learning Representations (ICLR)*. <https://openreview.net/forum?id=B1ckMDqlg> Poster.
- [24] Yuge Shi, N. Siddharth, Brooks Paige, and Philip H. S. Torr. 2019. Variational Mixture-of-Experts Autoencoders for Multi-Modal Deep Generative Models. In *Advances in Neural Information Processing Systems (NeurIPS)*.
- [25] Muhammad Shoaib, Hans Scholten, and P.J.M. Havinga. 2013. Towards Physical Activity Recognition Using Smartphone Sensors. In *2013 IEEE 10th International Conference on Ubiquitous Intelligence and Computing and 2013 IEEE 10th International Conference on Autonomic and Trusted Computing*. 80–87. <https://doi.org/10.1109/UIC-ATC.2013.43>
- [26] Masahiro Suzuki, Kohei Nakayama, and Yutaka Matsuo. 2016. Joint Multimodal Learning with Deep Generative Models. *arXiv preprint arXiv:1611.01891* (2016).
- [27] Timo Szytler, Heiner Stuckenschmidt, and Wolfgang Petrich. 2017. Position-aware Activity Recognition with Wearable Devices. *Pervasive and Mobile Computing* 38 (2017), 281–295. <https://doi.org/10.1016/j.pmcj.2016.10.012>
- [28] Cassia Valentini-Botinhao, Xin Wang, Shinji Takaki, and Junichi Yamagishi. 2016. Investigating RNN-based speech enhancement methods for noise-robust Text-to-Speech. In *Proceedings of the 9th ISCA Workshop on Speech Synthesis Workshop (SSW-9)*. 146–152. <https://doi.org/10.21437/SSW.2016-24>
- [29] Jindong Wang, Cuiling Lan, Chang Liu, Yidong Ouyang, Tao Qin, Wang Lu, Yiqiang Chen, Wenjun Zeng, and Philip S. Yu. 2022. Generalizing

- to Unseen Domains: A Survey on Domain Generalization. (2022). arXiv:cs.LG/2103.03097 <https://arxiv.org/abs/2103.03097>
- [30] Meichen Wang and Weihong Deng. 2018. Deep visual domain adaptation: A survey. *Neurocomputing* 312 (2018), 135–153.
- [31] Yuxuan Weng, Guoquan Wu, Tianyue Zheng, Yanbing Yang, and Jun Luo. 2024. Large Model for Small Data: Foundation Model for Cross-Modal RF Human Activity Recognition. In *Proceedings of the 22nd ACM Conference on Embedded Networked Sensor Systems (SenSys)*. ACM, 340–353. <https://doi.org/10.1145/3666025.3699349>
- [32] Garrett Wilson and Diane J Cook. 2020. A survey of unsupervised deep domain adaptation. *ACM Transactions on Intelligent Systems and Technology (TIST)* 11, 5 (2020), 1–46.
- [33] Huatao Xu, Pengfei Zhou, Rui Tan, and Mo Li. 2023. Practically Adopting Human Activity Recognition. In *Proceedings of the 29th Annual International Conference on Mobile Computing and Networking (MobiCom)*. ACM, 1285–1299. <https://doi.org/10.1145/3570361.3613299>
- [34] Bufang Yang, Lixing He, Neiweng Ling, Zhenyu Yan, Guoliang Xing, Xian Shuai, Xiaozhe Ren, and Xin Jiang. 2024. EdgeFM: Leveraging Foundation Model for Open-set Learning on the Edge. In *Proceedings of the 21st ACM Conference on Embedded Networked Sensor Systems (SenSys '23)*. Association for Computing Machinery, New York, NY, USA, 111–124. <https://doi.org/10.1145/3625687.3625793>
- [35] X. Yi, Z. Chen, M. Ma, X. Wu, and Y. Xu. 2021. Cross-modal Variational Auto-encoder for Content-based Micro-video Background Music Recommendation. *IEEE Transactions on Multimedia* (2021). to appear / early access.
- [36] George Zerveas, Srideepika Jayaraman, Dhaval Patel, Anuradha Bhamidipaty, and Carsten Eickhoff. 2021. A Transformer-based Framework for Multivariate Time Series Representation Learning. In *Proceedings of the 27th ACM SIGKDD Conference on Knowledge Discovery & Data Mining (KDD '21)*. Association for Computing Machinery, New York, NY, USA, 2114–2124. <https://doi.org/10.1145/3447548.3467401>
- [37] Han Zhao, Remi Tachet des Combes, Kun Zhang, and Geoffrey J. Gordon. 2019. On Learning Invariant Representation for Domain Adaptation. (2019). arXiv:cs.LG/1901.09453 <https://arxiv.org/abs/1901.09453>
- [38] Kaiyang Zhou, Ziwei Liu, Yu Qiao, Tao Xiang, and Chen Change Loy. 2023. Domain Generalization: A Survey. *IEEE Trans. Pattern Anal. Mach. Intell.* 45, 4 (April 2023), 4396–4415. <https://doi.org/10.1109/TPAMI.2022.3195549>
- [39] Rui Zhou, Yu Cheng, Songlin Li, Hongwang Zhang, and Chenxu Liu. 2025. DGSense: A Domain Generalization Framework for Wireless Sensing. (2025). <https://doi.org/10.48550/arXiv.2502.08155> arXiv preprint. arXiv:cs.LG/2502.08155 arXiv preprint.
- [40] Guozhen Zhu, Yuqian Hu, Weihang Gao, Wei-Hsiang Wang, Beibei Wang, and K. J. Ray Liu. 2025. CSI-Bench: A Large-Scale In-the-Wild Dataset for Multi-task WiFi Sensing. *arXiv preprint arXiv:2505.21866* (2025).